Target-Specific Gene Silencing of Layer-by-Layer Assembled Gold–Cysteamine/siRNA/PEI/HA Nanocomplex

Min-Young Lee,[†] Sang-Jun Park,[†] Kitae Park,[‡] Ki Su Kim,[†] Hwiwon Lee,[†] and Sei Kwang Hahn[†,‡,*]

[†]Department of Materials Science and Engineering, Pohang University of Science and Technology (POSTECH), San 31, Hyoja-dong, Nam-gu, Pohang, Kyungbuk 790-784, Korea, and [‡]School of Interdisciplinary Bioscience and Bioengineering, POSTECH, Pohang, Korea

ABSTRACT Target-specific intracellular delivery of small interfering RNA (siRNA) is regarded as one of the most important technologies for the development of siRNA therapeutics. In this work, a cysteamine modified gold nanoparticles (AuCM)/siRNA/polyethyleneimine (PEI)/hyaluronic acid (HA) complex was successfully developed using a layer-by-layer method for target-specific intracellular delivery of siRNA by HA receptor mediated endocytosis. Atomic force microscopic and zeta potential analyses confirmed the formation of a AuCM/siRNA/PEI/HA complex having a particle size of *ca.* 37.3 nm and a negative surface charge of *ca.* −12 mV. With a negligible cytotoxicity, AuCM/siRNA/PEI/HA complex showed an excellent target-specific gene silencing efficiency of *ca.* 70% in the presence of 50 vol % serum, which was statistically much higher than that of siRNA/Lipofectamine 2000 complex. In the competitive binding tests with free HA, dark-field bioimaging and inductively coupled plasma–atomic emission spectroscopy confirmed the target-specific intracellular delivery of AuCM/siRNA/PEI/HA complex to B16F1 cells with HA receptors. Moreover, the systemic delivery of AuCM/siRNA/PEI/HA complex using apolipoprotein B (ApoB) siRNA as a model drug resulted in a significantly reduced ApoB mRNA level in the liver tissue. Taken together, AuCM/siRNA/PEI/HA complex was thought to be developed as target-specific siRNA therapeutics for the systemic treatment of various liver diseases.

KEYWORDS: gold · siRNA · polyethyleneimine · hyaluronic acid · targeted delivery

Small interfering RNA (siRNA) is a short double-stranded RNA molecule, which can degrade the complementary mRNA suppressing the expression of disease-related genes.[1−3] Currently, siRNA is regarded as a new paradigm therapeutic agent for the treatment of various diseases caused by genetic disorder or viral infection. Nevertheless, the development of siRNA therapeutics has been impeded by the lack of efficient delivery systems of siRNA in the body.[4,5] Various kinds of materials, like cationic polymers,[6,7] lipids,[8] and nanoparticles,[9] have been exploited to overcome these technical hurdles. More recently, silica,[10] iron oxide,[11] and gold nanoparticles (AuNPs)[12−15] have been investigated extensively as emerging delivery carriers of siRNA. Especially, AuNPs have many advantages such as biocompatibility, simple synthesis, easily tunable size, facile surface modification, and versatile conjugation with biomolecules.[16−18] Elbakry *et al.* developed layer-by-layer assembled AuNPs incorporating siRNA with polyethyleneimine (PEI) for gene silencing applications.[13] PEI with a molecular weight (MW) of 25 kDa has been exploited as an efficient nonviral gene delivery carrier due to its strong endosomal escape capacity.[19] Song *et al*. also reported the preparation of PEI-capped AuNPs with a uniform structure and a narrow size distribution showing an effective reduction of targeted green fluorescent protein expression in MDA-MB-435s cells.[14] In addition, Lee *et al*. developed AuNP–siRNA conjugate *via* the formation of disulfide linkage which was coated with poly(β-amino ester) sequentially.[15] However, all these systems had two common limitations: positively charged surface characteristics and nonspecific delivery systems. The positive surface charge of nanoparticles might induce nonspecific binding with blood serum components resulting in aggregation and embolism in the body.[20] Moreover, nonspecific binding of positively charged nanoparticles to negatively charged cell membrane might induce nonspecific delivery of siRNA resulting in a drastically reduced therapeutic effect.[20]

To circumvent these problems, hyaluronic acid (HA) was introduced to the outer layer of siRNA delivery systems using AuNPs. HA has been exploited for a variety of medical applications including target-specific and long acting delivery of biopharmaceuticals and tissue engineering.[21−24] As a drug delivery carrier, HA has several advantages such as the negligible nonspecific interaction with serum components due to the polyanionic

* Address correspondence to skhanb@postech.ac.kr.

Received for review February 7, 2011 and accepted July 6, 2011.

Published online July 08, 2011
10.1021/nn2017793

characteristics,[25] and the highly efficient target-specific delivery to the liver tissues with HA receptors like cluster determinant 44 (CD44), hyaluronan receptor for endocytosis (HARE), and so on.[26−28] We previously reported the target-specific delivery of HA derivatives with an HA modification degree less than *ca.* 25 mol % to the liver using quantum dots (QDots).[29] In this work, a new target-specific siRNA delivery system was developed using a layer-by-layer assembled cysteamine-modified gold nanoparticles (AuCM)/siRNA/PEI/HA complex. The AuCM/siRNA/PEI/HA complex was characterized by transmission electron microscopy (TEM), atomic force microscopy (AFM), dynamic light scattering (DLS), and UV−vis spectra with MTT cytotoxicity tests. The target-specific intracellular delivery of the AuCM/siRNA/PEI/HA complex was assessed by competitive binding tests with free HA using dark-field bioimaging and inductively coupled plasma−atomic emission spectroscopy (ICP−AES). Then, *in vitro* target-specific gene silencing of the AuCM/siRNA/PEI/HA complex was investigated in the absence and presence of free HA. Finally, target-specific systemic delivery of the AuCM/siRNA/PEI/HA complex was carried out using apolipoprotein B (ApoB) siRNA and discussed for the treatment of various diseases in the liver with HA receptors.

RESULTS AND DISCUSSION

Preparation of AuCM/siRNA/PEI/HA Complex. Figure 1a shows a schematic representation for the preparation of the AuCM/siRNA/PEI/HA complex. AuCM was synthesized by reducing $HAuCl_4$ with $NaBH_4$ in the presence of cysteamine dihydrochloride as described elsewhere.[18] The formation of AuCM with a particle size of *ca.* 13 nm was confirmed by TEM image analysis (Figure 1b). The concentration of Au^{3+} in AuCM aqueous solution was measured to be 0.14 mg/mL by ICP−AES. Then, the molar concentration of AuCM was determined to be 10.45 nM by the calculation as reported elsewhere.[30] Then, negatively charged siRNA with a dimension of 5.5 nm × 2.0 nm was mixed with the positively charged AuCM. For efficient binding of siRNA to AuCM by electrostatic interaction, AuCM solution was added into siRNA solution in a dropwise manner and the mixture stirred slowly for 1 h. The molar ratio of AuCM to siRNA was optimized at a value of 1.57×10^{-2} to obtain a stable AuCM/siRNA complex with a high loading efficiency of siRNA (Supporting Information, Figure S1). The AuCM/siRNA complex was purified by centrifugation at 15000*g* for 15 min and redispersion in deionized (DI) water. The absorbance of the supernatant at 260 nm revealed that *ca.* 70% of siRNA in the mixture was attached to the AuCM, resulting in the loading of *ca.* 44 siRNA strands to one AuCM. PEI was selected as a polycation to be bound on the negatively charged AuCM/siRNA complex, because PEI can form a stable complex with nucleic acid by electrostatic interaction and has a strong endosomal escape capacity by the so-called proton sponge effect.[19] The purified AuCM/siRNA complex was added into 1 mg/mL of PEI solution. After stirring for 30 min, unbound PEI was removed by the centrifugation at 15000*g* for 15 min and redispersion in DI water four times. The unbound PEI required complete removal to exclude the complex formation of free PEI with consecutively added HA. The amount of PEI in the supernatant was determined by the CBQCA assay for the detection of amines, which revealed that the N/P ratio of PEI to siRNA was *ca.* 3.6 in the AuCM/siRNA/PEI complex. Finally, AuCM/siRNA/PEI/HA complex was obtained by the incubation with 4 mg/mL of HA solution for 30 min. Then, unbound HA was removed by the centrifugation at 15000*g* for 15 min and redispersion in DI water twice. The amount of HA in the supernatant was determined by the carbazole assay as described elsewhere,[31] which revealed that the weight ratio and the charge ratio of HA to PEI were *ca.* 15.7 and *ca.* 1.6, respectively.

Characterization of AuCM/siRNA/PEI/HA Complex. The layer-by-layer assembled AuCM/siRNA/PEI/HA complex was characterized by the analyses of TEM, AFM, DLS, and UV−vis spectra. First, the morphology of Au-based siRNA complexes was investigated by TEM as shown in Supporting Information, Figure S2 and Figure 1c. The electrostatic interaction between AuCM and siRNA resulted in the formation of AuCM/siRNA clusters. There was no further aggregation by the layer-by-layer assembly with PEI and HA. Figure 1c shows the TEM image of AuCM/siRNA/PEI/HA complex revealing the polyelectrolyte coating of AuCM/siRNA clusters. According to the vertical distance analysis of the Au-based siRNA complexes on AFM images, the particle size of AuCM, AuCM/siRNA, AuCM/siRNA/PEI, and AuCM/siRNA/PEI/HA complexes increased gradually with the mean diameters of 13.8 ± 3.2, 27.1 ± 8.9, 33.1 ± 10.5, and 37.3 ± 8.8 nm, respectively (Figure 2). The hydrodynamic size of the Au-based siRNA complexes was also analyzed by DLS. The hydrodynamic size of AuCM, AuCM/siRNA, AuCM/siRNA/PEI, and AuCM/siRNA/PEI/HA complexes increased gradually with mean diameters of 21.4 ± 3.2, 104.9 ± 6.6, 137.7 ± 5.6, and 165.5 ± 9.9 nm with low polydispersity indexes, respectively, (Supporting Information, Figure S3). The hydrodynamic size determined by DLS was larger than the particle size determined by AFM. The results can be explained by the fact that DLS analyzes the mean diameter calculated from the diffusional properties of dynamic nonspherical Au-based siRNA complexes in the hydrated state, whereas AFM analyzes the vertical height of Au-based siRNA complexes in the dried state.[32,33] The size and stability of nanoparticles are important factors for *in vivo* applications. Nanoparticles with a size in the range of 20−200 nm were reported to result in the reduced reticuloendothelial system (RES) uptake and the efficient passive tumor-targeting by enhanced permeation and

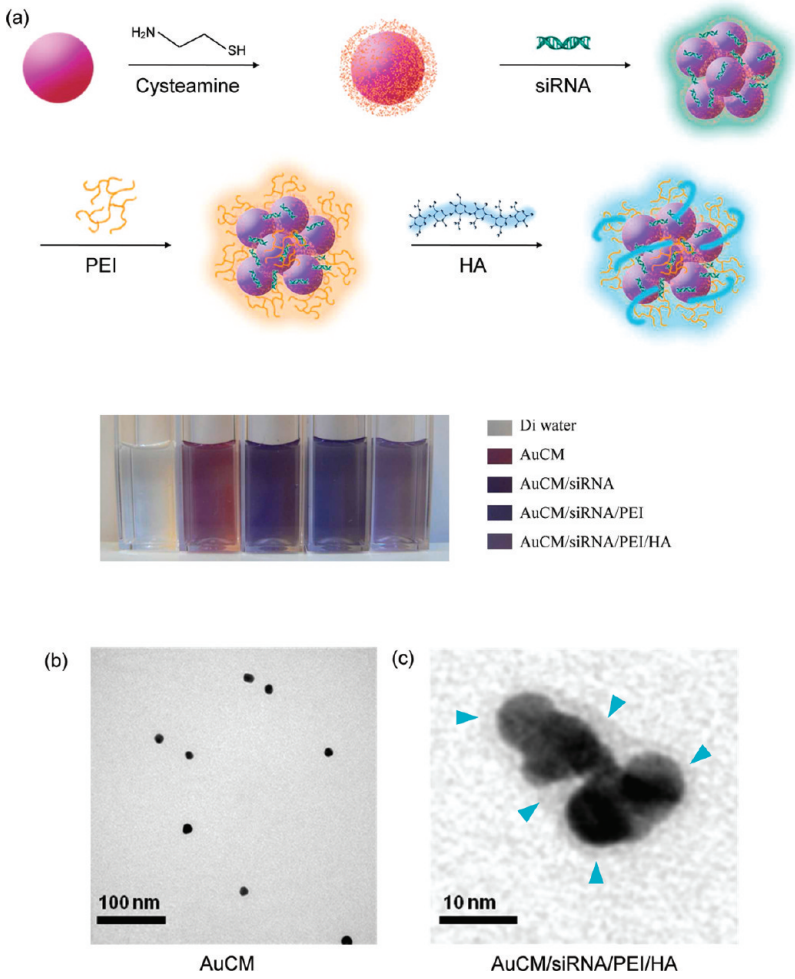

Figure 1. (a) Schematic representation for the preparation of layer-by-layer assembled cysteamine-modified gold nanoparticles (AuCM)/small interfering RNA (siRNA)/polyethyleneimine (PEI)/hyaluronic acid (HA) complex. Transmission electron microscopic images of (b) AuCM and (c) AuCM/siRNA/PEI/HA complex. Arrows indicate the polyelectrolyte-layers of PEI and HA encapsulating the AuCM/siRNA cluster.

retention (EPR).[34] The layer-by-layer complex formation was also confirmed by the surface charge analysis with a zeta-potential analyzer. The surface charge of AuCM, AuCM/siRNA, AuCM/siRNA/PEI, and AuCM/siRNA/PEI/HA complexes was changed alternately with the values of $+34.85 \pm 1.3$, -21.6 ± 0.8, $+22.5 \pm 3.3$, and -12.1 ± 1.5 mV, respectively (Figure 3a). The UV–vis spectra of AuCM, AuCM/siRNA, AuCM/siRNA/PEI, and AuCM/siRNA/PEI/HA complexes showed increased surface plasmon resonance (SPR) bands with the values of 527, 550, 554, and 559 nm. It was reported that the resonance curves shifted to higher wavelengths as AuNPs were aggregated or the thickness of the adsorbed molecules increased.[13,35] The considerable red shift from 527 to 550 nm and the slight broadening of AuCM/siRNA complex in SPR band confirmed that several AuCMs were assembled into an AuCM cluster by the electrostatic interaction with siRNA. It was reported that nanoclusters of metal particles were formed by self-assembly with polymers, and the size and physical properties of nanoclusters could be controlled by modulating the interaction between ligand-capped gold particles and polymers.[36,37] In contrast, the slight red shift in SPR band after coating with polyelectrolytes indicated that PEI and HA were layer-by-layer assembled without further aggregation of the AuCM/siRNA clusters (Figure 3b). The results were well matched with those by TEM image analysis (Supporting Information, Figure S2). All these results supported the successful formation of a layer-by-layer assembled AuCM/siRNA/PEI/HA complex.

Cellular Uptake of AuCM/siRNA/PEI/HA Complex. As shown in Supporting Information, Figure S4, the stability of AuCM/siRNA, AuCM/siRNA/PEI, and AuCM/siRNA/PEI/HA complexes was confirmed during the incubation with B16F1 cells in the medium containing serum for up to 24 h. Although AuCM/siRNA and AuCM/siRNA/PEI complexes gradually aggregated and precipitated with increasing time in the cell culture medium containing serum, the AuCM/siRNA/PEI/HA complex was very stable without aggregation and precipitation even after incubation for 24 h. Because of the stiff and rodlike

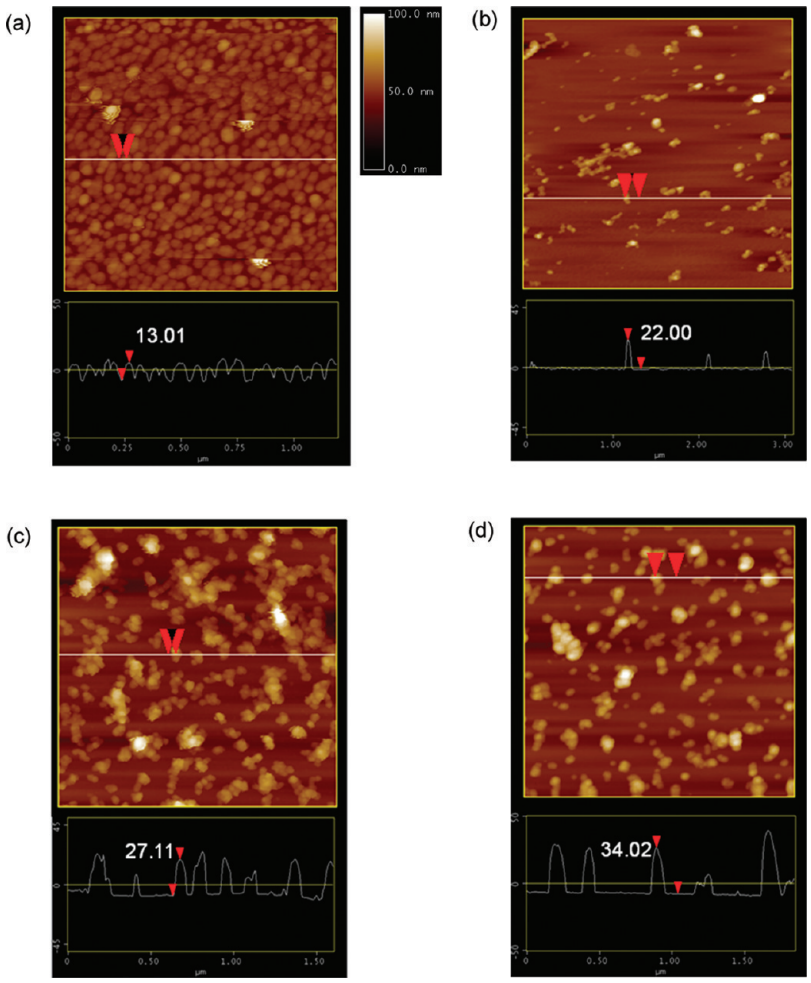

Figure 2. Atomic force microscopic images for the particle size analysis of (a) AuCM, (b) AuCM/siRNA, (c) AuCM/siRNA/PEI, and (d) AuCM/siRNA/PEI/HA complexes.

morphology of siRNA with a length of *ca.* 5.5 nm, it can be difficult for siRNA to wrap around AuCM with a dimension of *ca.* 13.4 nm.[13] Accordingly, AuCM/siRNA complex might be unstable and the exposed siRNA might be degraded by nuclease in the cell culture medium containing serum. For the case of PEI coated NPs, PEI can interact strongly with serum components resulting in the aggregation of a AuCM/siRNA/PEI complex. In contrast, the AuCM/siRNA/PEI/HA complex showed the enhanced stability in the presence of serum, which might be attributed to the outer-layer of HA. It is well-known that HA can minimize the nonspecific interaction with serum components.[25] Then, the cellular uptake of Au-based siRNA complexes was visualized by TEM analysis after incubation for 24 h. Figure 4a shows the attachment of aggregated AuCM/siRNA complexes to the membrane of B16F1 cells. In the case of AuCM/siRNA/PEI complexes, some of the complexes were bound to the cell membrane and others were up-taken to the cells in the form of large aggregates (Figure 4b). On the other hand, AuCM/siRNA/PEI/HA complexes were taken up by B16F1 cells without large aggregates and well distributed in the cytosol (Figures 4c,d). The size of AuNPs was reported to strongly influence the cellular uptake of AuNPs.[38] The enhanced serum stability and the effective cellular uptake by HA receptor mediated endocytosis might be attributed to the HA in the outer layer of AuCM/siRNA/PEI/HA complex.

***In Vitro* Gene Silencing of AuCM/siRNA/PEI/HA Complex.** Before gene silencing application, the cytocompatibility of AuCM/siRNA, AuCM/siRNA/PEI, and AuCM/siRNA/PEI/HA complexes was confirmed in B16F1 cells by MTT assay with the cell viability higher than 90% (Supporting Information, Figure S5). Then, *in vitro* gene silencing of Au-based siRNA complexes was investigated using luciferase-specific siRNA (siLuc) and nonspecific siRNA in B16F1 cells. The gene silencing efficiency was *ca.* 30% for the AuCM/siLuc complex and *ca.* 50% for both AuCM/siLuc/PEI and AuCM/siLuc/PEI/HA complexes in the presence of 10 vol % serum (Figure 5a). To simulate *in vivo* circumstance, the gene silencing efficiency was also assessed in the presence of 50 vol % serum. The gene silencing efficiency of AuCM/siLuc and AuCM/siLuc/PEI complexes decreased slightly in comparison with those in the presence of 10 vol % serum. However, the AuCM/siLuc/PEI/HA complex resulted in

an increased gene silencing efficiency up to the range of 70−80%, which might be ascribed to the serum stability of the AuCM/siLuc/PEI/HA complex. The results

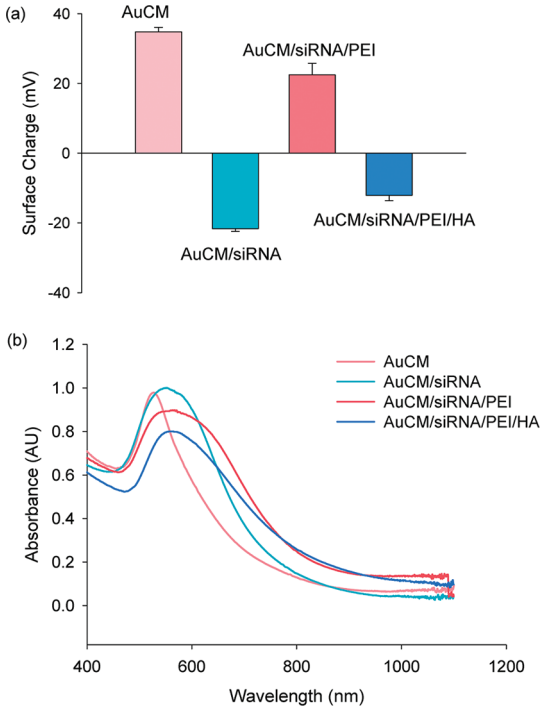

Figure 3. (a) Zeta potential analysis of Au-based siRNA complexes in DI water. The results represent mean ± standard deviation (n = 3). (b) UV−vis spectra of Au-based siRNA complexes.

can be supported by the previous report that serum proteins are necessary for the stabilization of Au-based complexes.[13] For further assessment, the gene silencing of the AuCM/siRNA/PEI/HA complex was carried out using vascular endothelial growth factor-specific siRNA (siVEGF) in B16F1 cells. There have been many reports on the therapeutic application of siVEGF for the treatment of cancer.[20] The gene silencing efficiency of AuCM/siVEGF/PEI/HA complex was evaluated by real time-polymerase chain reaction (RT-PCR) for intracellular VEGF mRNA levels in the presence of 50 vol % serum. The AuCM/siVEGF/PEI/HA complex resulted in *ca.* 70% reduction of the VEGF mRNA level which was much higher than the *ca.* 20% by siVEGF/Lipofectamine 2000 complex (Figure 5b). It is well-known that the gene silencing efficiency of siRNA complexed with cationic polymers such as PEI decreases drastically in the presence of 50 vol % serum.[39] To alleviate these problems, we previously reported the development of siRNA/reducible PEI-*b*-HA complex.[20] Nevertheless, the gene silencing efficiency of siRNA/(PEI-SS)-b-HA complex was lower in the presence of 50 vol % serum than that of 10 vol % serum. Considering all these results, the AuCM/siRNA/PEI/HA complex was thought to be more effectively exploited for *in vivo* applications than the conventional gene silencing systems.

Target Specific Gene Silencing of AuCM/siRNA/PEI/HA Complex. The target-specific cellular uptake of AuCM/siRNA/PEI/HA complex by HA receptor mediated endocytosis was investigated by dark-field bioimaging (Figure 6) and

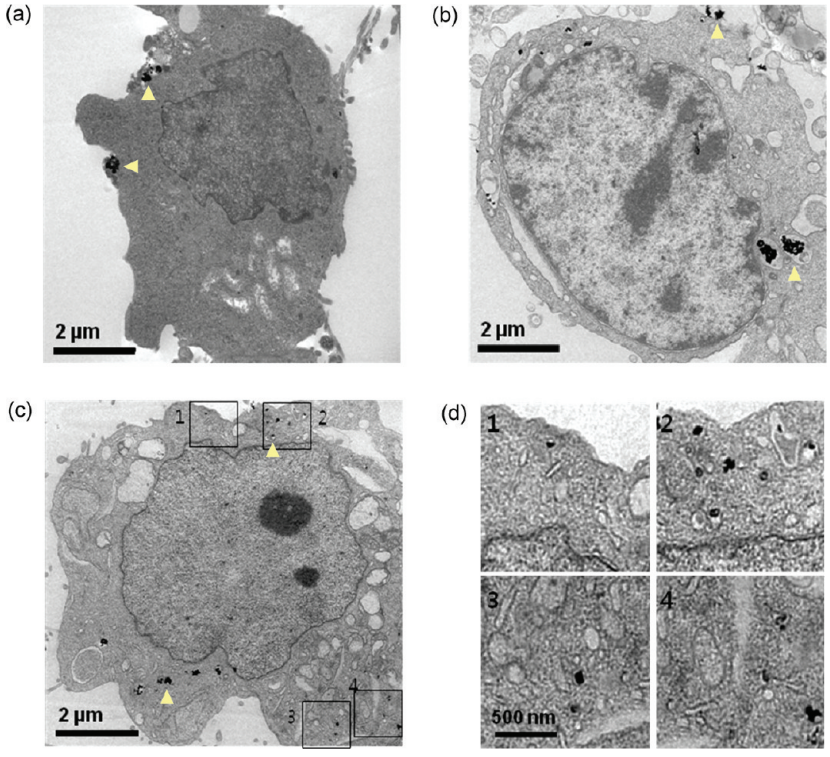

Figure 4. Transmission electron micrographs of B16F1 cells after incubation with (a) AuCM/siRNA, (b) AuCM/siRNA/PEI, and (c) AuCM/siRNA/PEI/HA complexes, and (d) the magnified image of panel c.

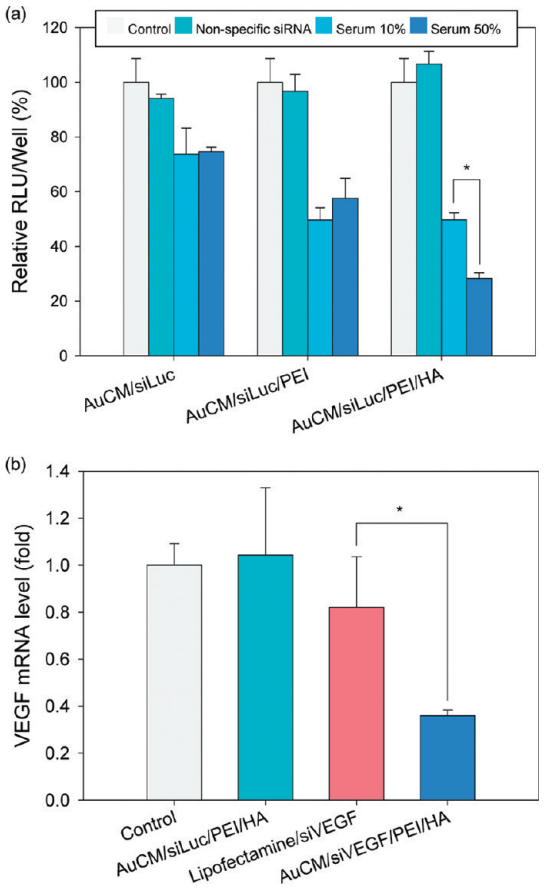

Figure 5. (a) Luciferase gene silencing in B16F1 cells by Au-based siRNA complexes: control, Au-based siRNA complexes using nonspecific siRNA, and antiluciferase siRNA in the presence of 10 vol % or 50 vol % serum from left to right. (b) VEGF gene silencing by AuCM/siVEGF/PEI/HA complex in the presence of 50 vol % serum with the comparison to the control, AuCM/nonspecific siRNA/PEI/HA complex, and siVEGF/Lipofectamine complex. The results represent mean ± standard deviation ($n = 3$, (*) $P < 0.05$).

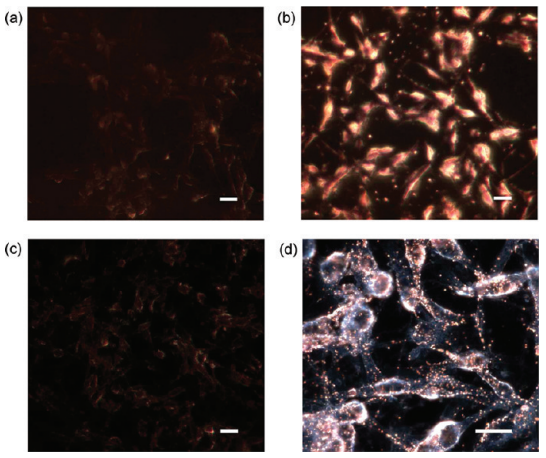

Figure 6. Dark-field bioimages of B16F1 cells (a) without treatment as a control and with the treatment of AuCM/siRNA/PEI/HA complex (b) in the absence of free HA and (c) in the presence of free HA (2 mg/mL) for competitive binding tests, and (d) the magnified image of panel b. Scale bars indicate 20 μm.

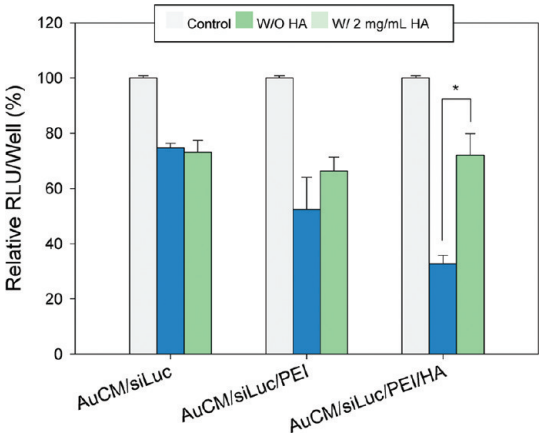

Figure 7. Target-specific gene silencing in the presence of 50 vol % serum: Control along with Au-based siRNA complexes without and with free HA (2 mg/mL) from left to right. The results represent mean ± standard deviation ($n = 3$, (*) $P < 0.05$).

ICP–AES (Supporting Information, Figure S6). For competitive binding tests, B16F1 cells with HA receptors such as CD44 and LYVE-1[40] were preincubated in a medium containing 50 vol % serum with and without free HA (2 mg/mL) for 1 h, and treated with AuCM/siRNA/PEI/HA complex. After 24 h incubation and washing with PBS thrice, bioimages were taken to assess dark-field light scattering of AuNPs in B16F1 cells.[41] Morphologies of cells were clearly visualized in the dark by the bright scattering of AuNPs uptaken to the cells in the absence of free HA (Figure 6b,d). However, there was no or little dark-field light scattering for the cases of the untreated control (Figure 6a) and preincubation with free HA (Figure 6c). In addition, the quantitative analysis of the competitive cellular uptake by ICP–AES confirmed that the AuCM/siRNA/PEI/HA complex was more internalized to B16F1 cells than AuCM/siRNA and AuCM/siRNA/PEI complexes in the absence of free HA (Supporting Information, Figure S6). While the cellular uptake of AuCM/siRNA and AuCM/siRNA/PEI complexes was slightly changed in the presence of free HA, that of the AuCM/siRNA/PEI/HA complex was drastically reduced with increasing HA concentrations. To confirm the target-specific gene silencing by HA receptor-mediated endocytosis of the AuCM/siRNA/PEI/HA complex, the gene silencing tests were also carried out in the absence and presence of free HA (2 mg/mL). As shown in Figure 7, the gene silencing efficiency in the presence of free HA was statistically lower than that in the absence of free HA. The results were well matched with the competitive binding tests using dark-field bioimaging and ICP–AES. The outer-layer of HA in AuCM/siRNA/PEI/HA complex was thought to contribute to the target-specific gene silencing after the HA receptor mediated endocytosis in B16F1 cells with HA receptors.

Target-Specific Systemic Gene Silencing of AuCM/siRNA/PEI/HA Complex. On the basis of the target specificity of HA

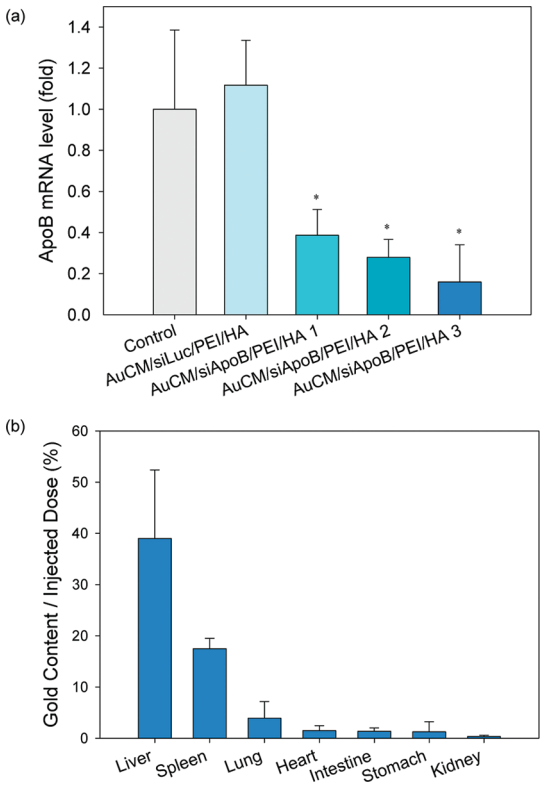

Figure 8. (a) Apolipoprotein B (ApoB) mRNA levels after target-specific systemic gene silencing with the control and three kinds of AuCM/siApoB/PEI/HA complexes at the doses of 0.45, 0.90, and 1.8 nmol of siRNA/mouse. The results represent mean ± standard deviation (n = 4, (∗) $P < 0.05$ *versus* the control). (b) The percentage of AuNPs to injected dose in various organs after tail vein injection of AuCM/siRNA/PEI/HA complex. The results represent mean ± standard deviation (n = 4).

to the liver and *in vitro* gene silencing test results, we carried out the target-specific systemic delivery of AuCM/siRNA/PEI/HA complex using ApoB-specific siRNA (siApoB). ApoB is the essential protein for the formation of low-density lipoproteins (LDL) which is responsible for carrying cholesterol to tissues and expressed mostly in the liver.[42,43] It was reported that the secretion of hepatitis C virus (HCV), the leading cause of liver cirrhosis, was highly dependent on lipoproteins, and the high level of ApoB was known to be related with heart diseases.[43,44] After tail-vein injection to Balb/c mice, the AuCM/siApoB/PEI/HA complex was effectively delivered to the liver, which resulted in a drastically reduced ApoB mRNA level down to *ca.* 20% in a dose-dependent manner (Figure 8a). The results might be ascribed to the negligible nonspecific interaction with serum components and the target-specific delivery to the liver tissues by HA in the outer-layer of AuCM/siApoB/PEI/HA complex. The comparative studies could not be performed with AuCM/siRNA and AuCM/siRNA/PEI complexes because the complexes were aggregated and precipitated in PBS, while the AuCM/siRNA/PEI/HA complex was very stable in PBS even after 24 h. Furthermore, after the tail-vein injection of the AuCM/siRNA/PEI/HA complex, the biodistribution was investigated by ICP−AES.[45] Most of the complexes accumulated in the liver (*ca.* 40% of injected dose) and spleen (*ca.* 17% of injected dose) in accordance with the systemic gene silencing test results. On the basis of these results taken together, AuCM/siRNA/PEI/HA complex was thought to be applied as novel target-specific siRNA therapeutics to the treatment of various liver diseases such as chronic hepatitis, liver cirrhosis, and liver cancer.

CONCLUSION

A layer-by-layer assembled AuCM/siRNA/PEI/HA complex was successfully developed for target-specific gene silencing applications. The AuCM/siRNA/PEI/HA complex had a mean particle size of 37.3 ± 8.8 nm with a negative surface charge of −12.1 ± 1.5 mV. TEM, dark-field bioimaging, and ICP−AES analyses confirmed the effective cellular uptake of the AuCM/siRNA/PEI/HA complex to B16F1 cells by HA receptor-mediated endocytosis. With a negligible cytotoxicity, the gene silencing efficiency of AuCM/siRNA/PEI/HA was extraordinarily high in the range of 70−80% in the presence of 50 vol % serum. The HA in the outer layer of the AuCM/siRNA/PEI/HA complex was thought to contribute to the stability and the target-specific gene silencing. Moreover, target-specific systemic delivery of the AuCM/siRNA/PEI/HA complex resulted in a drastically reduced ApoB mRNA level down to *ca.* 20% in a dose-dependent manner. The AuCM/siRNA/PEI/HA complex might be successfully exploited for target-specific treatment of various liver diseases.

MATERIALS AND METHODS

Materials. Hyaluronic acid (HA) with a molecular weight (MW) of 100 kDa was purchased from Lifecore Co. (Chaska, MN). Branched polyethyleneimine (PEI) with a MW of 25 kDa, chloroauric acid ($HAuCl_4$), and sodium borohydride ($NaBH_4$) were obtained from Sigma-Aldrich (St. Louis, MO). Cysteamine dihydrochloride was purchased from Tokyo Chemical Industry Co. (Tokyo, Japan) and dimethyl sulfoxide (DMSO) from Junsei Chemical Co. (Tokyo, Japan). B16F1 cells of murine melanoma were obtained from Korean Cell Line Bank (Seoul, Korea). Dulbecco's Modified Eagle's Medium (DMEM), fetal bovine serum (FBS), antibiotics, phosphate buffered saline (PBS), Trizol, and Lipofectamine 2000 reagent were purchased from Invitrogen Co. (Carlsbad, CA). MTT assay kit, pVMC luciferase plasmid, lysis solution, and luciferase assay reagents were obtained from Promega Co. (Madison, WI), and jetPEI was obtained from Polyplus-transfection Co. (New York, NY). First strand cDNA synthesis kit and Taq DNA polymerase were purchased from Takara Bio Inc. (Shiga, Japan). Anti-pVMC-Luc siRNA (siLuc), anti-VEGF siRNA (siVEGF), and antiapolipoprotein B siRNA (siApoB) were purchased from Bioneer Co. (Daejeon, Korea). The sequences of siLuc are 5′-UUGUUUUGGAGCGAAAdTdT-3′ (sense) and

5′-UUUCGCUCCAAAACAAdTdT-3′ (antisense). The sequences of siVEGF are 5′-AUGUGAAUGCAGACCAAAGAATTdTdT-3′ (sense) and 5′-UUCUUUGGUCUGCAUUCACAATTdTdT-3′ (antisense). The sequences of siApoB are GUCAUCACACUGAAUACCAAUdTdT-3′ (sense) and 5′-AUUGGUAUUCAGUGUGAUGACdTdT-3′ (antisense). All reagents were used without further purification.

Synthesis of Cysteamine-Modified Gold Nanoparticles. AuCMs were prepared by the reduction of $HAuCl_4$ with $NaBH_4$ in the presence of cysteamine dihydrochloride as described elsewhere.[18] Briefly, 800 μL of cysteamine hydrochloride aqueous solution (0.2 M) was added to 80 mL of $HAuCl_4$ aqueous solution (1.4 mM). After stirring for 20 min, 2 mL of $NaBH_4$ aqueous solution (1 mM) was added to the solution in a dropwise manner, which stirred at room temperature for 12 h. The resulting solution was poured into a prewashed dialysis membrane tube (MWCO 10 kDa) and dialyzed against DI water for 12 h. The concentration of Au^{3+} in AuCM aqueous solution was measured by ICP−AES (ICAP 6000 series, Thermo scientific, Soeul, Korea). The molar concentration of AuCM was determined by the calculation as reported elsewhere.[30]

Preparation of the AuCM/siRNA/PEI/HA Complex. The AuCM/siRNA/PEI/HA complex was prepared using the layer-by-layer method. First, 4.5 mL of 10.45 nM AuCM solution was added to 0.5 mL of 6 μM siRNA solution in a dropwise manner. After stirring for 1 h, the AuCM/siRNA complex was purified by centrifugation at 15000*g* for 15 min and redispersion in DI water twice. The binding efficiency of siRNA to AuCM was analyzed by measuring the absorbance of the supernatant of AuCM/siRNA complex at 260 nm with an Uvikon 941 spectrophotometer (Kontron Instruments GmbH, Germany). The amount of siRNA was determined using a standard calibration curve. The AuCM/siRNA complex was redispersed in 1 mg/mL of PEI solution. After stirring for 30 min, the AuCM/siRNA/PEI complex was purified by centrifugation at 15000*g* for 15 min and redispersion in DI water four times. The amount of PEI bound to the AuCM/siRNA complex was analyzed with an ATTO-TAG CBQCA amine-derivatization kit (Invitrogen Co., Carlsbad, CA) following the manufacturer's protocol. Finally, the AuCM/siRNA/PEI complex was redispersed in 4 mg/mL of HA solution. After stirring for 30 min, AuCM/siRNA/PEI/HA complex was purified by centrifugation at 15000*g* for 15 min and redispersion in DI water twice. The amount of HA bound to the AuCM/siRNA/PEI complex was analyzed by the carbazole assay as described elsewhere.[31]

Characterization of AuCM/siRNA/PEI/HA Complex. The morphology and particle size of AuCM, AuCM/siRNA, AuCM/siRNA/PEI, and AuCM/siRNA/PEI/HA complexes were analyzed by TEM (Hitachi, Tokyo, Japan) and AFM (VEECO Instrument Co., New York, NY). For the TEM analysis, each 10 μL drop of the Au-based siRNA complex solutions was placed on 300 mesh copper TEM grids with a carbon film, air-dried, and analyzed with the TEM operating at 300 kV. For the AFM analysis, each 100 μL of the Au-based siRNA complex solutions was placed on a silicon wafer. The silicon wafer was air-dried for 5 h and then the remaining solution on the silicon wafer was blown away using a syringe pump. The average complex particle size was determined from the vertical distance of 100 particles of AuCM, AuCM/siRNA/PEI, and AuCM/siRNA/PEI/HA complexes, and 60 particles of AuCM/siRNA complex on the AFM images. The hydrodinamic diameter and the surface charge of Au-based siRNA complexes in DI water were characterized by DLS (Zetasizer Nano, Malvern Instrument Co., UK). The Au-based siRNA complexes were also analyzed with an UV−vis spectrophotometer (S-3100, Scinco Co., Seoul, Korea).

TEM Imaging for the Cellular Uptake. For the TEM imaging, B16F1 cells were grown in 100 mm culture dishes to 90% confluency. Cells were treated with AuCM/siRNA, AuCM/siRNA/PEI, and AuCM/siRNA/PEI/HA complexes in DMEM with 50 vol % FBS. After incubation for 24 h, cells were washed with PBS thrice, detached, pelleted by centrifugation, fixed with 2% glutaraldehyde in cacodylate buffer overnight, and rinsed with 0.1 M cacodylate buffer. Postfixation was performed for 100 min in 1% osmium tetroxide at 4 °C. After several washing steps with 0.1 M cacodylate buffer, the sample was embedded in agarose and dehydrated in a graded series of ethanol (70, 80, 90, 95, and 100 vol %). Then, the sample was embedded in Epon. Ultrathin sections with a thickness of *ca.* 70 nm were imaged at 20 kV using a TEM (JEM-1011, JEOL LTD, Tokyo, Japan).

***In Vitro* Gene Silencing.** B16F1 cells were dispersed into 24-well plate at a population of 2×10^4 cells/well and incubated at 37 °C for 24 h. B16F1 cells were pretransfected with PVMC-Luc plasmid as described elsewhere.[20] Briefly, cells were pretransfected with 0.5 mL of serum-free DMEM containing 1 μg of PVMC-Luc vector using a jetPEI reagent following the product instruction. After incubation for 3 h and the subsequent washing with PBS several times, the Au-based siLuc complexes were transfected at a siRNA concentration of 100 nM for gene silencing in DMEM containing 10 vol % and 50 vol % FBS, respectively. After incubation for 24 h, the transfected cells were lysed with a lysis buffer of 1 wt % Triton X-100, and then 10 μL of the lysed solution was mixed with 25 μL of luciferase assay solution. In comparison to the gene silencing by nonspecific siRNA, the luciferase activity was measured with a luminescence microplate reader (Luminoskan Ascent, Lab systems, Germany). Furthermore, the target-specific gene silencing of AuCM/siRNA/PEI/HA complex in B16F1 cells was investigated by the competitive gene silencing tests in DMEM containing 50 vol % FBS and 2 mg/mL of free HA. For VEGF gene silencing tests, AuCM/siVEGF/PEI/HA complex was prepared using the same protocol as described above. B16F1 cells were seeded on a 6-well plate at a density of 1×10^5 cells/well and incubated at 37 °C for 24 h. AuCM/siVEGF/PEI/HA complex was transfected to the cells in DMEM containing 50 vol % FBS for 24 h in comparison with AuCM/nonspecific siLuc/PEI/HA complex and siVEGF/Lipofectamine 2000 complex following the manufacturer's protocol. The cells were lysed with Trizol and RNA was extracted from the cells. Then, 1 μg of the RNA was reversely transcribed to cDNA using the first strand cDNA synthesis kit following the manufacturer's protocol. The VEGF mRNA level was measured by RT-PCR with Taq DNA polymerase and normalized with the GAPDH mRNA level. The primer sequences were as follows. GAPDH: forward, 5′-AGGCCGGTGCTGAGTATGTC-3′; and reverse, 5′-TGCCTGCTTCACCACCTTCT-3′. VEGF: forward, 5′-GGAGATCCTTCGAGGZGCACTT-3′; and reverse, 5′-GGCGATTTAGCAGCAGATATAAGAA-3′. PCR parameters were as follows: initial denaturation for 5 min at 95 °C followed by 40 cycles of 30 s at 95 °C and 30 s at 53 °C.

Dark-Field Bioimaging. B16F1 cells were seeded on 8-well culture slides (Bedford, MA) at a density of 1×10^4 cells/well and incubated for 24 h. Then, culture medium was exchanged with DMEM containing 50 vol % FBS with and without 2 mg/mL of free HA. After incubation for 1 h, the cells were treated with AuCM/siRNA/PEI/HA complex at 37 °C for 24 h. The B16F1 cells without treatment were used as a negative control. The cells were washed with PBS thrice, fixed with 4 vol % paraformaldehyde, and analyzed by dark-field bioimaging (Axioplan 2 Microscope, Carl Zeiss, Germany).

Target-Specific Systemic Gene Silencing. The systemic target-specific gene silencing of AuCM/siApoB/PEI/HA complex was assessed by measuring the ApoB mRNA level using RT-PCR and normalizing with GAPDH mRNA level. Four groups of male Balb/c mice at an average age of 5 weeks were treated with the control of PBS and three kinds of AuCM/siApoB/PEI/HA complexes at the doses of 0.45, 0.90, and 1.8 nmol of siRNA/mouse in 0.2 mL of PBS, respectively. After 24 h, the mice were sacrificed and the dissected livers were lysed with Trizol to extract RNA from the liver cells. Then, 1 μg of the RNA was reversely transcribed to cDNA using the first strand cDNA synthesis kit following the manufacturer's protocol. The cDNA was amplified using Taq DNA polymerase. The primer sequences were as follows. GAPDH: forward, 5′-AGGCCGGTGCTGAGTATGTC-3′; and reverse, 5′-TGCCTGCTTCACCACCTTCT-3′. ApoB: forward, 5′-TTTTCCTCCCAGATTTCAAGG-3′; and reverse, 5′-TCCAGCATTGGTATTCAGTGTG-3′.

Biodistribution. Male Balb/c mice at an average age of 5 weeks were treated with the negative control of PBS and AuCM/siLuc/PEI/HA complex at a dose of 1.8 nmol siRNA/mouse in 0.2 mL of PBS. After 24 h, the mice were sacrificed and the dissected organ samples were dried. The Au^{3+} content was determined by ICP−AES.[45] The organ samples were dissolved in 10 mL of freshly prepared aqua regia with heating until the solution became transparent. After evaporation, 10 mL of 50% HCl and

10 mL of 50% HNO_3 were added, filtered using a filter paper, and diluted to the final volume of 50 mL with DI water. The samples (n = 4) were analyzed by ICP–AES (ICAP 6000 series, Thermo scientific, Soeul, Korea). Samples treated as described above but without addition of AuNPs were used as the control for background subtraction. Using the Au peak at 267.6 nm, all standards were made with gold(III) chloride at a concentration of 0.1, 0.5, 1, 5, and 10 ppm. All measurements of standards and samples were carried out with the ICP–AES system performed at a RF power of 1350 W, a pump rate of 50 rpm, and a nebulizer gas flow of 0.6 lpm Ar.

Statistical Analysis. The data are expressed as means ± standard deviation from several separate experiments. Statistical analysis was carried out *via* *t*-test using the software of SigmaPlot 10.0, and a value for $P < 0.05$ was considered statistically significant.

Acknowledgment. This research was supported by the Converging Research Center Program through the National Research Foundation of Korea (NRF) funded by the Ministry of Education, Science and Technology (2009-0081871). This research was also supported by the R&D Program of MKE/KEIT (10035159).

Supporting Information Available: Additional figures as discussed in the text. This material is available free of charge *via* the Internet at http://pubs.acs.org.

REFERENCES AND NOTES

1. Elbashir, S. M.; Harborth, J.; Lendeckel, W.; Yalcin, A.; Weber, K.; Tuschl, T. Duplexes of 21-Nucleotide RNAs Mediate RNA Interference in Cultured Mammalian Cells. *Nature* **2001**, *411*, 494–499.
2. Qin, X. F.; An, D. S.; Chen, I. S.; Baltimore, D. Inhibiting HIV-1 Infection in Human T Cells by Lentiviral-Mediated Delivery of Small Interfering RNA against CCR5. *Proc. Natl. Acad. Sci. U.S.A.* **2003**, *100*, 183–188.
3. Schiffelers, R. M.; Ansari, A.; Xu, J.; Zhou, Q.; Tang, Q.; Storm, G.; Molema, G.; Lu, P. Y.; Scaria, P. V.; Woodle, M. C. Cancer siRNA Therapy by Tumor Selective Delivery with Ligand-Targeted Sterically Stabilized Nanoparticle. *Nucleic Acids Res.* **2004**, *32*, e149.
4. Aagaard, L.; Rossi, J. J. RNAi Therapeutics: Principles, Prospects and Challenges. *Adv. Drug Delivery Rev.* **2007**, *59*, 75–86.
5. White, P. J. Barriers to Successful Delivery of Short Interfering RNA after Systemic Administration. *Clin. Exp. Pharmacol. Physiol.* **2008**, *35*, 1371–1376.
6. Boussif, O.; Lezoualc'h, F.; Zanta, M. A.; Mergny, M. D.; Scherman, D.; Demeneix, B.; Behr, J.-P. A Versatile Vector for Gene and Oligonucleotide Transfer into Cells in Culture and *in Vivo*: Polyethylenimine. *Proc. Natl. Acad. Sci. U.S.A.* **1995**, *92*, 7297–7301.
7. Kim, H. J.; Ishii, A.; Miyata, K.; Lee, Y.; Wu, S.; Oba, M.; Nishiyama, N.; Kataoka, K. Introduction of Stearoyl Moieties into a Biocompatible Cationic Polyaspartamide Derivative, PAsp(DET), with Endosomal Escaping Function for Enhanced siRNA-Mediated Gene Knockdown. *J. Controlled Release* **2010**, *145*, 141–148.
8. Zou, S.; Scarfo, K.; Nantz, M. H.; Hecker, J. G. Lipid-Mediated Delivery of RNA Is More Efficient than Delivery of DNA in Nondividing Cells. *Int. J. Pharm.* **2010**, *389*, 232–243.
9. Fay, F.; Quinn, D. J.; Gilmore, B. F.; McCarron, P. A.; Scott, C. J. Gene Delivery Using Dimethyldidodecyl Ammoniumbromide-Coated PLGA Nanoparticles. *Biomaterials* **2010**, *31*, 4214–4222.
10. Chen, A. M.; Zhang, M.; Wei, D.; Stueber, D.; Taratula, O.; Minko, T.; He, H. Co-delivery of Doxorubicin and Bcl-2 siRNA by Mesoporous Silica Nanoparticles Enhances the Efficacy of Chemotherapy in Multidrug-Resistant Cancer Cells. *Small* **2009**, *5*, 2673–2677.
11. Boyer, C.; Priyanto, P.; Davis, T. P.; Pissuwan, D.; Bulmus, V.; Kavallaris, M.; Teoh, W. Y.; Amal, R.; Carroll, M.; Woodward, R.; *et al.* Antifouling Magnetic Nanoparticles for siRNA Delivery. *J. Mater. Chem.* **2010**, *20*, 255–65.
12. Rosi, N. L.; Giljohann, D. A.; Thaxton, C. S.; Lytton-Jean, A. K. R.; Han, M. S.; Mirkin, C. A. Oligonucleotide-Modified Gold Nanoparticles for Intracellular Gene Regulation. *Science* **2006**, *312*, 1027–1030.
13. Elbakry, A.; Zaky, A.; Liebl, R.; Rachel, R.; Goepferich, A.; Breunig, M. Layer-by-layer Assembled Gold Nanoparticles for siRNA Delivery. *Nano Lett.* **2009**, *9*, 2059–2064.
14. Song, W. J.; Du, J. Z.; Sun, T. M.; Zhang, P. Z.; Wang, J. Gold Nanoparticles Capped with Polyethyleneimine for Enhanced siRNA Delivery. *Small* **2010**, *6*, 239–246.
15. Lee, J. S.; Green, J. J.; Love, K. T.; Sunshine, J.; Langer, R.; Anderson, D. G. Gold, Poly(β-amino ester) Nanoparticles for Small Interfering RNA Delivery. *Nano Lett.* **2009**, *9*, 2402–2406.
16. Ghosh, P.; Han, G.; De, M.; Kim, C. K.; Rotello, V. M. Gold Nanoparticles in Delivery Applications. *Adv. Drug Delivery Rev.* **2008**, *60*, 1307–1315.
17. Li, N.; Larson, T.; Nguyen, H. H.; Sokolov, K. V.; Ellington, A. D. Directed Evolution of Gold Nanoparticle Delivery to Cells. *Chem. Commun.* **2010**, *46*, 392–394.
18. Niidome, T.; Nakashima, K.; Takahashi, H.; Niidome, Y. Preparation of Primary Amine-Modified Gold Nanoparticles and their Transfection Ability into Cultivated Cells. *Chem. Commun.* **2004**, *17*, 1978–1979.
19. Godbey, W. T.; Wu, K. K.; Mikos, A. G. Poly(ethylenimine) and its Role in Gene Delivery. *J. Controlled Release* **1999**, *60*, 149–160.
20. Park, K.; Lee, M. Y.; Kim, K. S.; Hahn, S. K. Target Specific Tumor Treatment by VEGF siRNA Complexed with Reducible Polyethyleneimine–Hyaluronic Acid Conjugate. *Biomaterials* **2010**, *31*, 5258–5265.
21. Laurent, T. C.; Laurent, U. B. G.; Fraser, J. R. E. The Structure and Function of Hyaluronan: An Overview. *Immunol. Cell. Biol.* **1996**, *74*, A1–7.
22. Kong, J. H.; Oh, E. J.; Chae, S. Y.; Lee, K. C.; Hahn, S. K. Long Acting Hyaluronate–Exendin 4 Conjugate for the Treatment of Type 2 Diabetes. *Biomaterials* **2010**, *31*, 4121–4128.
23. Oh, E. J.; Park, K.; Kim, K. S.; Kim, J.; Yang, J. A.; Kong, J. H. Target Specific and Long-Acting Delivery of Protein, Peptide, and Nucleotide Therapeutics Using Hyaluronic Acid Derivatives. *J. Controlled Release* **2010**, *141*, 2–12.
24. Yeom, J.; Bhang, S. H.; Kim, B. S.; Seo, M. S.; Hwang, E. J.; Cho, I. H.; Park, J. K.; Hahn, S. K. Effect of Cross-Linking Reagents for Hyaluronic Acid Hydrogel Dermal Fillers on Tissue Augmentation and Regeneration. *Bioconjugate Chem.* **2010**, *21*, 240–247.
25. Ito, T.; Iida-Tanaka, T.; Niidome, K.; Kawano, K.; Kubo, T.; Yoshikawa, Z.; Sato, Y. Koyama. Hyaluronic Acid and its Derivative as a Multifunctional Gene Expression Enhancer: Protection from Nonspecific Interactions, Adhesion to Targeted Cells, and Transcriptional Activation. *J. Controlled Release* **2006**, *112*, 382–388.
26. Aruffo, A.; Stamenkovic, I.; Melnick, M.; Underhill, C. B.; Seed, B. CD44 is the Principal Cell Surface Receptor for Hyaluronate. *Cell* **1990**, *61*, 1303–1313.
27. Entwistle, J.; Hall, C. L.; Turley, E. A. HA Receptors: Regulators of Signalling to the Cytoskeleton. *J. Cell. Biochem.* **1996**, *61*, 569–577.
28. Zhou, B.; Weigel, J. A.; Fauss, L.; Weigel, P. H. Identification of the Hyaluronan Receptor for Endocytosis (HARE). *J. Biol. Chem.* **2000**, *275*, 37733–37741.
29. Kim, K. S.; Hur, W.; Park, S. J.; Hong, S. W.; Choi, J. E.; Goh, E. J.; Yoon, S. K.; Hahn, S. K. Bioimaging for Targeted Delivery of Hyaluronic Acid Derivatives to the Livers in Cirrhotic Mice Using Quantum Dots. *ACS Nano* **2010**, *4*, 3005–3014.
30. Liu, X.; Atwater, M.; Wang, J.; Huo, Q. Extinction Coefficient of Gold Nanoparticles with Different Sizes and Different Capping Ligands. *Colloids Surf. B* **2007**, *58*, 3–7.
31. Song, J.-M.; Im, J.-H.; Kang, J.-H.; Kang, D.-J. A Simple Method for Hyaluronic Acid Quantification in Culture Broth. *Carbohydr. Polym.* **2009**, *78*, 633–634.
32. Lee, S. K.; Han, M. S.; Asokan, S.; Tung, C.-H. Effective Gene Silencing by Multilayered siRNA-Coated Gold Nanoparticles. *Small* **2011**, *7*, 364–370.

33. Pecora, R. Dynamic Light Scattering Measurement of Nanometer Particles in Liquids. *J. Nanopart. Res.* **2000**, *2*, 123–131.
34. Schmalenberg, K. E.; Frauchiger, L.; Nikkhouy-Albers, L.; Uhrich, K. E. Cytotoxicity of a Unimolecular Polymeric Micelle and Its Degradation Products. *Biomacromolecules* **2001**, *2*, 851–855.
35. Schneider, G.; Decher, G. Functional Core/Shell Nanoparticles *via* Layer-by-Layer Assembly. Investigation of the Experimental Parameters for Controlling Particle Aggregation and for Enhancing Dispersion Stability. *Langmuir* **2008**, *24*, 1778–1789.
36. Ofir, Y.; Samanta, B.; Rotello, V. M. Polymer and Biopolymer Mediated Self-Assembly of Gold Nanoparticles. *Chem. Soc. Rev.* **2008**, *37*, 1814–1825.
37. Boal, A. K.; Ilhan, F.; Derouchey, J. E.; Thurn-Albrecht, T.; Russell, T. P.; Rotello, V. M. Self-Assembly of Nanoparticles into Structured Spherical and Network Aggregates. *Nature* **2000**, *404*, 746–748.
38. Chithrani, B. D.; Ghazani, A. A.; Chan, W. C. W. Determining the Size and Shape Dependence of Gold Nanoparticle Uptake into Mammalian Cells. *Nano Lett.* **2006**, *6*, 662–668.
39. Shim, M. S.; Kwon, Y. J. Dual Mode Polyspermine with Tunable Degradability for Plasmid DNA and siRNA Delivery. *Biomaterials* **2011**, *32*, 4009–4020.
40. He, Y.; Rajantie, I.; Ilmonen, M.; Makinen, T.; Karkkainen, M. J.; Haiko, P.; Salven, P.; Alitalo, K. Preexisting Lymphatic Endothelium but Not Endothelial Progenitor Cells Are Essential for Tumor Lymphangiogenesis and Lymphatic Metastasis. *Cancer Res.* **2004**, *64*, 3737–3740.
41. Nam, J.; Won, N.; Jin, H; Chung, H.; Kim, S. pH-Induced Aggregation of Gold Nanoparticles for Photothermal Cancer Therapy. *J. Am. Chem. Soc.* **2009**, *131*, 13639–13645.
42. McCormick, S. P.; Ng, J. K.; Véniant, M.; Borén, J.; Pierotti, V.; Flynn, L. M.; Grass, D. S.; Connolly, A.; Young, S. G. Transgenic Mice that Overexpress Mouse Apolipoprotein B: Evidence that the DNA Sequences Controlling Intestinal Expression of the Apolipoprotein B Gene are Distant from the Structural Gene. *J. Biol. Chem.* **1996**, *271*, 11963–11970.
43. Ihara, Y.; Yoshimura, M.; Miyoshi, E.; Nishikawa, A.; Sultan, A. S.; Toyosawa, S.; Ohnishi, A.; Suzuki, M.; Yamamura, K.; Ijuhin, N.; *et al*. Ectopic Expression of *N*-Acetylglucosaminyltransferase III in Transgenic Hepatocytes Disrupts Apolipoprotein B Secretion and Induces Aberrant Cellular Morphology with Lipid Storage. *Proc. Natl. Acad. Sci. U.S.A.* **1998**, *95*, 2526–2530.
44. Soutschek, J.; Akinc, A.; Bramlage, B.; Charisse, K.; Constien, R.; Donoghue, M.; Elbashir, S.; Geick, A.; Hadwiger, P.; Harborth, J.; *et al*. Therapeutic Silencing of an Endogenous Gene by Systemic Administration of Modified siRNAs. *Nature* **2004**, *432*, 173–178.
45. De Jong, W. H.; Hagens, W. I.; Krystek, P.; Burger, M. C.; Sips, A. J.; Geertsma, R. E. Particle Size-Dependent Organ Distribution of Gold Nanoparticles after Intravenous Administration. *Biomaterials* **2008**, *29*, 1912–1919.